AD NUMBER

AD456365

NEW LIMITATION CHANGE

TO

Approved for public release, distribution unlimited

FROM

Distribution authorized to U.S. Gov't. agencies and their contractors; Administrative/Operational Use; DEC 1964. Other requests shall be referred to Office of Naval Research, Arlington, VA 22217.

AUTHORITY

CFSTI per ONR ltr, 11 Mar 1966

DEFENSE DOCUMENTATION CENTER

FOR

SCIENTIFIC AND TECHNICAL INFORMATION

CAMERON STATION ALEXANDRIA, VIRGINIA

DDC

FEB 15 1965

DDC-IRA B

HYDRONAUTICS, incorporated
research in hydrodynamics

HYDRONAUTICS, Incorporated

HIGH FREQUENCY FATIGUE OF METALS AND THEIR CAVITATION DAMAGE RESISTANCE

By·

A. Thiruvengadam

December 1964

HYDRONAUTICS, Incorporated

TABLE OF CONTENTS

LIST OF FIGURES

HYDRONAUTICS, Incorporated

-111-

NOTATION

Q	Quality factor
f_n	Natural frequency
Δf	Width of the resonance curve at half the maximum amplitude
λ	Wave length of sound
c	Velocity of sound
E	Modulus of elasticity
ρ	Density
η	Fatigue notch sensitivity
K_f	Ratio of unnotched fatigue strength to notched fatigue strength
K_t	Theoretical stress concentration factor
ϵ_{max}	Maximum strain
ζ_{max}	Maximum amplitude
σ_a	Stress amplitude
S_e	Strain energy
σ	True stress
ϵ_p	True plastic strain
n	Strain hardening exponent
ϵ_f	True ultimate fracture strain
σ_f	True ultimate fracture stress
σ_f'	Auxiliary true ultimate fracture stress

HYDRONAUTICS, Incorporated

SUMMARY

Recent experiments (1,2) have shown that the plastic strain energy (as given by the area of the stress-strain diagram obtained from a simple tensile test) is at present the most significant criterion for cavitation damage resistance of metals. Since the strain rates involved in the cavitation damage process were several orders of magnitude higher than that in a simple tensile test from which the strain energy was derived, the above result is surprising.

In order to confirm the preceding result, high frequency fatigue tests at 14.2 kcs (at the same frequency used for cavitation damage tests) were conducted for five metals. Recently Morrow (3) used plastic strain energy as a criterion for finite fatigue life and derived a relationship connecting stress to fracture and number of cycles to fracture by making use of true ultimate tensile strength and the strain hardening exponent. He showed reasonable correlation with forty sets of data. Good correlation is also obtained with the present experiments and Morrow's theory if the strain hardening exponent is reduced by about fifteen percent for all the five metals. This result confirms that plastic strain energy is a good criterion even at high strain rates.

Another result revealed by the present study is the influence of corrosion. Recently (7) it was shown that cavitation damage in a corrosive environment increases greatly while the contributions from direct electrochemical corrosion could not

account for this great increase. It was postulated that the increased damage must come principally from the deterioration of the strength due to corrosion fatigue, but there were serious doubts whether corrosion could play any significant role at these high frequencies. Present experiments show that fatigue strength can be reduced significantly for SAE 1020 steel in 3 percent NaCl solution even at high frequencies, thus confirming the earlier speculations.

INTRODUCTION

Recent attempts to characterize the cavitation damage resistance of metals by a common mechanical property have shown that the most significant correlation could be established with the strain energy of the material in the steady state zone (1,2). This strain energy is given by the fracture energy per unit volume of the metal as obtained from the area of the stress-strain diagram from a simple tensile test. The cavitation damage process takes place at strain rates several orders of magnitude higher than the simple tensile test which gives the fracture energy at relatively low strain rates. It seemed surprising that the fracture energy at such low strain rates could still represent the energy absorbing capacity of metals under the highly transient stresses produced by the cavitation bubble collapse. Some experimental verification was needed to clarify the strain rate effects on fracture energy of metals in order to explain these results.

During these studies the thought provoking investigations of Morrow (3) using plastic strain energy as a criterion for finite fatigue life came to the attention of the author. Morrow successfully related the plastic strain energy per cycle to the static true strain energy for forty sets of data including carbon steels, alloy steels, nickel based alloys, various aluminum alloys, beryllium and brass. This prompted the present investigations in which the fatigue tests at a frequency of 14 kcs were conducted following the pioneering work of Gaines (4), Mason (5) and Neppiras (6). Morrow's analysis was extended to the high frequency fatigue tests to see how much the strain rate effects interact and modify the analysis. As a result of this analysis, it has been found that a good correlation between the theory and experiments can be obtained if the value of the strain hardening exponents are reduced by 15 percent from the static result. This shows that the strain rate effects are relatively small when energy is used as a criterion for the fracture mechanism.

Another important aspect clarified by these investigations is the interaction of the corrosive environment on cavitation damage. It has been observed that the damage rates in a corrosive environment are much higher than those observed in a relatively non-corrosive environment (7). The electrochemical corrosion estimated by four different methods could not account for this increase in rate of damage. On the basis of these findings, it was postulated that the major contribution to the increase of rate of damage in a corrosive environment should

come mainly from the change in the fatigue properties of the material in that corrosive environment. However, a popular point of view has hypothesized that under cavitation conditions the surface material was being removed so rapidly that there was insufficient time for appreciable corrosive weakening of the surface. The present investigations include the test results for one metal (1020 SAE steel) in 3 percent NaCl solution and these results show that fatigue properties of non-resistant metal in a corrosive environment can be drastically changed even under very high frequencies.

EXPERIMENTAL APPARATUS

The experimental technique adopted for the present investigations consists of oscillating a metallic rod at its resonant longitudinal frequency. This frequency was selected to be the same as that used for previous cavitation damage tests. This technique enables the utilization of the magnetostriction apparatus used previously for cavitation damage tests. Gaines (4) who introduced the idea of using magnetostriction oscillators for cavitation damage testing also suggested the use of the same equipment for fatigue testing as well. He, in fact, carried out a few fatigue tests in his apparatus. However, this technique did not gain popularity until Mason (5) and Neppiras (6) successfully used exponential and stepped velocity transformers, thereby making the technique more versatile, because high strains can be produced on any metal with moderate power. A detailed discussion of the various aspects involved in this method is given by Neppiras (6, 8).

HYDRONAUTICS, Incorporated

In essence, the apparatus consists of a magnetostriction transducer, an oscillator, an amplifier, a power supply, a voice coil, an oscilloscope and a frequency counter (Figure 1). An exponential velocity transformer is attached to the magneto-striction nickel transducer stack. The characteristics of the entire system are shown in Figure 2 for three resonant frequencies. The resonant frequency of the system can be varied by varying the length of that portion of the velocity transformer from the nodal support to the free end by means of extension rods. The amplitude is monitored by a suitable voltage pick-up coil located approximately midway between the node and the antinode. A permanent magnet is used in the immediate vicinity of the coil to increase the induced voltage. This induced voltage is proportional to the displacement amplitude and the instrument is calibrated by measuring the displacement at the antinode with a filar microscope. The accuracy of these measurements is discussed later.

A detailed study of the transducer system showed that the best quality factor was obtained at 14.2 kcs and hence this frequency was selected for fatigue tests. The quality factor is defined as the ratio of usable energy stored in the system to the total input energy and is given by (9),

$$Q = \frac{\sqrt{3}}{\pi} \frac{f_n}{\Delta f} \qquad [1]$$

where f_n is the resonant frequency and Δf is the width of the resonant curve at half of the maximum amplitude.

DESIGN OF TEST SPECIMENS

General Aspects

The basic principle of the design of the high frequency fatigue specimens is as follows: When a longitudinal vibration of a half wave length of a metallic rod is produced by means of an oscillator, the maximum strain is produced at the node while the maximum velocity and displacement are produced at the antinodes at either end of the rod (Figure 3). If a notch is produced at the node, then the strain is further amplified at the node. It is necessary to amplify the strains by means of a notch because of the power limitations of the driving oscillator. There are two other unwanted side effects due to this notch, namely: (i) the fatigue notch sensitivity and (ii) the change in resonant frequency. These two effects will be discussed subsequently.

The main idea is to attach a half wave length of the metallic rod to the free end of the exponential horn and to vibrate it at the best frequency selected from considerations of the quality factor. The half wave length can be experimentally determined by adjusting the rod length to resonate at the best frequency. An accurate determination of this length and frequency will give the value of velocity of sound for each of the metals tested by the relationship

$$\lambda f_n = c \qquad\qquad [2]$$

where

λ   is the wave length,

f_n is the resonant frequency, and

c   is the velocity of sound.

The modulus of elasticity also can be calculated after deter-
mining the density of the metals by the conventional water dis-
placement method, by

$$E = \rho c^2 \qquad\qquad [3]$$

where

E   is the modulus of elasticity

ρ   is the density of the metal.

Table 1 gives the physical properties thus determined for each
of the six metals under investigation.

Notch Sensitivity

As pointed out earlier, a notch was provided at the node
to induce the required strains. It is known that fatigue is
sensitive to notches depending upon the geometry of the notches.
This effect is characterized by a factor η known as notch
sensitivity

$$\eta = \frac{K_f - 1}{K_t - 1} \qquad\qquad [4]$$

where

$$K_f = \frac{\text{un-notched fatigue strength}}{\text{notched fatigue strength}} \text{, and}$$

K_t = the theoretical stress concentration factor.

Experimental information on η as a function of notch radius is available for steels and aluminum alloys in References 10 and 11. The notch radius was selected so that η would be as close to unity as possible. The same notch radius was adopted for both Tobin Bronze and Monel since no experimental data were readily available for these metals. Next, the theoretical stress concentration factors for round bars may be found from Reference 12. The dimensions of the notch selected are shown in Figure 4(a). A photograph of the 1020 SAE steel specimen is shown in Figure 4(b).

The stresses are calculated as follows: The maximum strain at the node for a uniform rod in sinusoidal vibration is given by

$$\epsilon_{max} = \frac{2\pi \, \zeta_{max}}{\lambda} \qquad [5]$$

where ζ_{max} is the maximum amplitude. The stress amplitude σ_a is given by

$$\sigma_a = \epsilon_{max} \cdot E \qquad [6]$$

HYDRONAUTICS, Incorporated

For the present design, the theoretical stress concentration factor from Reference 12 is 1.65 and the area ratio is 4. Hence the magnification factor, M is 4 times 1.65 and the stress amplitude is given by

$$\sigma_a = 6.6 \frac{2\pi}{\lambda} \zeta_{max} \cdot E \qquad [7]$$

Effect of Notch on Resonant Frequency

Another effect of the notch is to lower the resonant frequency slightly. This can be rectified by reducing the length of the fatigue specimen after a few trial and error experiments. This modified length can also be predicted by an approximate theory following Neppiras (6). However, the change in wave length due to the notch remains within 10 percent as shown in Table 1 and this can be taken into account in the calculation of stresses.

EXPERIMENTAL PROCEDURE AND ACCURACY

Amplitude Measurement and Determination of Maximum Stress

As pointed out earlier, the maximum amplitude at the antinode where the fatigue specimen is attached is monitored by means of a calibrated voice coil located as shown in Figure 1. Since the fatigue specimen forms a half wave length, its addition does not change either the frequency or the calibration. The voltage developed by the coil was of the order of 35 volts, corresponding to an amplitude of 2.5×10^{-3} inch and hence

For the present design, the theoretical stress concentration factor from Reference 12 is 1.65 and the area ratio is 4. Hence the magnification factor, M is 4 times 1.65 and the stress amplitude is given by

$$\sigma_a = 6.6 \, \frac{2\pi}{\lambda} \, \xi_{max} \cdot E \qquad [7]$$

Effect of Notch on Resonant Frequency

Another effect of the notch is to lower the resonant frequency slightly. This can be rectified by reducing the length of the fatigue specimen after a few trial and error experiments. This modified length can also be predicted by an approximate theory following Neppiras (6). However, the change in wave length due to the notch remains within 10 percent as shown in Table 1 and this can be taken into account in the calculation of stresses.

EXPERIMENTAL PROCEDURE AND ACCURACY

Amplitude Measurement and Determination of Maximum Stress

As pointed out earlier, the maximum amplitude at the anti-node where the fatigue specimen is attached is monitored by means of a calibrated voice coil located as shown in Figure 1. Since the fatigue specimen forms a half wave length, its addition does not change either the frequency or the calibration. The voltage developed by the coil was of the order of 35 volts, corresponding to an amplitude of 2.5×10^{-3} inch and hence

maintain constant amplitude. (An automatic amplitude control has
been designed for future studies). The determination of this
fracture time is no problem especially above ten million cycles
since it would take about 12 minutes to reach this value. It
would take 20 hours to reach a billion cycles and this time is
designated as "run-out" time. (Run-out is defined as the number
of cycles at which the test is discontinued even if the specimen
does not fracture).

Fabrication of Test Pieces

Figure 4(a) shows the dimensional tolerances required for
the fabrication of the specimens. The specimens were ground to
the final dimensions from a 3/4 inch round bar stock for all
the five metals except for SAE 1020 steel. The specimens were
in the annealed condition and of the same heat as was used for
previous cavitation damage tests and stress-strain measurements.
Cavitation damage specimens and tensile test specimens were pre-
pared from the same bar stock of the metals. The fatigue speci-
mens for SAE 1020 steel were prepared from 1/2 inch round bar
stock; however, the cavitation damage and tensile test data
were not available for the same heat.

As soon as these specimens were machined they were coated
with a corrosion protective film * and stored. This film was
removed with methanol before each test. For this initial limited
program, only ten specimens were tested for each metal except
for SAE 1020 steel for which about 30 specimens were used.

---

* Zip Spray No. 2 by Zip Abrasive Company of Cleveland, Ohio.

Cooling and Environmental Control

Without outside cooling, the fatigue specimens become excessively hot near the node due to the high dynamic strains. To avoid this unwanted heating, a constant temperature, close to atmospheric temperature, was maintained by immersing the specimen in a constant temperature bath. This bath provided simultaneously the corrosive or non-corrosive environment as required. For the present experiments, the fatigue specimens were immersed in a beaker full of either distilled water or methanol, which was kept at constant temperature $\pm 2^{\circ}F$. by means of another cooling jacket through which tap water was circulated. For one set of experiments with SAE 1020 steel, 3 percent NaCl solution was used as the environmental bath to provide the corrosive environment. This arrangement is shown in Figure 6.

RESULTS AND ANALYSIS

Results

Figure 7 shows the results of these tests for five metals, namely:

       (a)   1100-F Aluminum

       (b)   2024-T4 Aluminum

       (c)   Tobin Bronze

       (d)   Monel

       (e)   316 Stainless Steel.

The dark circles show the results of tests in methanol, whereas all the other tests were conducted in distilled water. These results show the negligible effect of corrosion by distilled water.

Analysis

As pointed out in the introduction, the main aim of these investigations is to obtain a quantitative insight into the strain rate effects on the fracture energy of these metals. The following analysis, originally due to Morrow (3), has been quite useful for this purpose.

Brief review of Morrow's Theory: The following important assumptions are made in this theory.

1. Plastic strain energy is a criterion for finite fatigue life.

2. The total plastic strain energy to fracture increases as the alternating stress is reduced in a completely reversed fatigue test. Specifically, it has been assumed that this quantity is inversely proportional to the fourth power of the alternating stress.

3. The plastic strain energy per cycle can be related to the static true stress-strain curve.

The theoretical justifications, the experimental verification and the limitations of these assumptions are discussed in detail by Morrow in his original paper. The derivation of the essential equations will be touched upon only briefly in this report.

HYDRONAUTICS, Incorporated

The plastic strain energy up to fracture per unit volume is given by

$$S_e = \int_0^{\epsilon_f} \sigma \, d\epsilon_p \qquad [8]$$

and

$$\sigma \propto \epsilon_p^n \qquad [9]$$

where σ is the true stress corresponding to a true plastic strain of ϵ_p (see Figure 8), and n is the strain hardening exponent.

Now

$$\sigma = \sigma_f' \left(\frac{\epsilon_p}{\epsilon_f}\right)^n \qquad [10]$$

where σ_f' is the true fracture stress corresponding to the fracture strain ϵ_f. In some materials, deviation from linearity in a log-log plot of true stress versus true strain occurs past necking (probably due to the triaxial stresses present in the necked region). For this reason, σ_f' has been defined as the stress obtained by extrapolating the straight line region as shown in Figure 8(b) to the strain at fracture. The experimentally measured value would be σ_f.

Substituting Equation [10] in [8] and integrating gives

$$S_e = \frac{1}{1+n} \sigma_f' \epsilon_f \qquad [11]$$

Similarly the plastic strain energy, or the work done per cycle Δw is

$$\Delta w = 2 \int_0^{\Delta \epsilon_p} \sigma \, d \, \epsilon_p$$

$$= \frac{2}{1 + n} \sigma_a \, \Delta \epsilon_p \qquad [12]$$

Assuming that Δw remains constant for the entire test at a given stress level, the work done up to fracture W_f is given by

$$N_f \Delta w = W_f \qquad [13]$$

The dependence of W_f on σ_a was evaluated by a combination of a dimensional analysis due to Liu (13) and the Griffith crack theory. There is a region of plastic deformation around each crack. Assuming these regions are geometrically similar, the stored plastic energy will depend upon the square of the crack length.

Thus

$$\frac{W_2}{W_1} = \left(\frac{L_2}{L_1} \right)^2 \qquad [14]$$

Invoking Griffith's theory,

$$L\sigma^2 = \text{constant} \qquad [15]$$

and hence

$$\frac{L_2}{L_1} = \left(\frac{\sigma_a}{\sigma_1}\right)^{-2} \qquad [16]$$

Combining Equations [14] and [16], one gets

$$\frac{\sigma_2}{\sigma_1} = \left(\frac{W_2}{W_1}\right)^{-\frac{1}{4}} \qquad [17]$$

Hence

$$\frac{\sigma_a}{\sigma_f{}'} = \left(\frac{W_f}{S_e}\right)^{-\frac{1}{4}} \qquad [18]$$

Combining Equations [11], [12], [13] and [18], one obtains

$$2N_f\left(\frac{\sigma_a}{\sigma_f{}'}\right)^5 \frac{\Delta\epsilon_p}{\epsilon_f} = 1 \qquad [19]$$

$$\frac{\Delta\epsilon_p}{\epsilon_f} = \left(\frac{\sigma_a}{\sigma_f{}'}\right)^{\frac{1}{n}} \qquad [20]$$

Now from [19] and [20]

$$\sigma_a = \sigma_f{}'\left(2N_f\right)^{-\frac{n}{1+5n}} \qquad [21]$$

In logarithmic form

$$\log \sigma_a = \log \sigma_f' - \frac{n}{1 + 5n} \log (2N_f) \qquad [22]$$

Morrow found this analysis for completely reversed, constant amplitude uniaxial fatigue to agree with the trends in forty sets of fatigue data of metals.

The above analysis was used to check the experimental data of the present high frequency fatigue tests. The values of σ_f' and n as obtained from true stress-strain diagrams for these five metals are shown in Table 2. It was found that Equation [22] fits the experimental data for all of the five metals tested, if the value of n used in Equation [22] is fifteen percent less than the actual values as obtained from tests. A comparison between the curves predicted from the above analysis using 85 percent of the value of n and the experimental data are shown in Figure 9. This agreement shows that the high strain rates involved in the present testing method has not substantially changed the plastic energy required to fracture the metal in fatigue. This conclusion is very significant in explaining why the strain energy gives the most significant correlation with cavitation damage resistance.

Influence of Corrosion

One of the serious limitations to the above analysis is the influence of corrosive environment. It is known that cavitation damage is greatly increased in a corrosive liquid. For a typical

-18-

case of NaCl solutions and SAE 1020 steel, this relationship is
reproduced from Reference 7 in Figure 10. It was pointed out
in that reference that the estimated electrochemical corrosion
could not account for the large increase in damage and there-
fore the fatigue strength of the metal must have deteriorated
due to corrosion. There were some doubts as to whether the
fatigue strength could be affected so greatly under such high
frequencies. To clarify this point, a few experiments were
conducted using SAE 1020 steel. Figure 11 shows the results
with methanol, distilled water, and 3 percent NaCl solution as
liquid environments. One can easily notice the detrimental ef-
fect of corrosion on the fatigue strength of steel even at this
high frequency.

An analysis similar to the one above gives the following
equation for this steel in a non-corrosive environment.

$$\log \sigma_a = \log 1.25 \times 10^5 - \frac{0.07}{1 + 5 \times 0.07} \log 2N_f \qquad [23]$$

The effect of corrosion can be represented quantitatively by
means of the following equation.

$$\log \sigma_a = \log \sigma_f' - \frac{n}{1 + 5n} \log 2N_f - CN_f \qquad [24]$$

where C is an empirical corrosion fatigue factor. For the pres-
ent results, n turns out to be 4×10^{-10} as shown in Figure 12.
It is believed that a deeper understanding of this corrosion
factor C would eventually lead to a quantitative representation
of corrosive interaction in cavitation damage.

CONCLUSIONS

Based on the results of these investigations, the following conclusions may be stated.

1. The plastic strain energy correlation found to be successful to represent cavitation damage and low frequency fatigue, can equally be used for correlating high frequency data. This result shows that strain rate effects may not introduce deviations greater than 10 to 20 percent in the strain hardening exponent. This result is significant in explaining the correlations obtained with cavitation damage (1, 2).

2. Fatigue strength of non-resistant metals in a corrosive environment can be significantly changed even under high frequencies. This tends to explain the earlier findings with regard to the very high increase in cavitation erosion in a corrosive liquid (7).

REFERENCES

1. Thiruvengadam, A., "A Unified Theory of Cavitation Damage," Trans. ASME, Vol. 85, Jour. Basic Eng., pp. 365-377, September 1963.

2. Thiruvengadam, A., and Waring, S., "Mechanical Properties of Metals and Their Cavitation Damage Resistance," HYDRO-NAUTICS Incorporated Technical Report 233-5, June 1964.

3. Morrow, Jo Dean, "An Investigation of Plastic Strain Energy as a Criterion for Finite Fatigue Life," The Garrett Corporation Report, Phoenix, Arizona, 1960.

4. Gaines, N., "A Magnetostriction Oscillator Producing Intense Audible Sound and Some Effects Obtained," Physics, Vol. 3, No. 5, pp. 209-229, 1932.

5. Mason, W. P., "Internal Friction and Fatigue in Metals at Large Strain Amplitude," The Jour. Acous. Soc. America, Vol. 28, No. 6, pp. 1207-1218, 1956.

6. Neppiras, E. A., "Techniques and Equipment for Fatigue Testing at Very High Frequencies," Proc. ASTM, Vol. 59, pp. 691-709, 1959.

7. Waring, S., Preiser, H. S., and Thiruvengadam, A., "On the Role of Corrosion in Cavitation Damage," HYDRONAUTICS, Incorporated Technical Report 233-4, February 1964.

8. Neppiras, E. A., "Metal Fatigue at High Frequency," Proc. Physical Soc., B., (London) Vol. 70, p. 393, 1957.

9. Jensen, J. W., "Damping Capacity - Its Measurement and Significance," Report of Investigations, Bureau of Mines, U. S. Dept. of Interior, 1959.

10. Harris, W. J., "Metallic Fatigue," Pergamon Press, Inc., p. 22, 1961.

HYDRONAUTICS, Incorporated

11. Grover, H. J., "Fatigue Notch Sensitivities of Some
     Aircraft Materials," Proc. Am. Soc. Testing Materials,
     Vol. 50, pp. 717-729, 1950.

12. Lyman, T., ed., Gerlach, C. H., assoc. ed., Metals Hand-
     book, 1954 Supplement, The Am. Soc. for Metals, p. 98,
     1954.

13. Liu, H. W., University of Illinois, Personal Communication
     to Morrow (3).

TABLE 1

Required Design Parameters for High Frequency
Fatigue Specimens as Determined Experimentally

Metal	Velocity of Sound fps	Density gms/cm³	Modulus of Elasticity psi	Wave Length inches	Modified Wave Length of Notched Speci-men (inches)	Resonant Frequency
1020 Mild Steel	16700	7.85	29.0×10^6	14.0	13.0	14,290
1100-F Aluminum	16700	2.70	10.0×10^6	14.0	13.2	14,210
2024-T4 Aluminum	16700	2.70	10.0×10^6	14.0	13.2	14,200
316 Stainless Steel	16300	7.98	28.4×10^6	13.6	12.6	14,220
Monel	14650	8.84	25.4×10^6	12.3	11.2	14,300
Tobin Bronze	10950	8.41	11.8×10^6	9.2	8.3	14,200

TABLE 2

The Values Of σ_f' And n For The Five Metals Analyzed

Metal	σ_f' Kips	n	85% n	Strain Energy S_e in Kips
316 Stainless Steel	120	0.10	0.085	35
Monel	110	0.08	0.068	24
Tobin Bronze	83	0.10	0.85	17
2024-T4 Aluminum	81	0.13	0.11	13
1100-F Aluminum	26	0.07	0.06	4
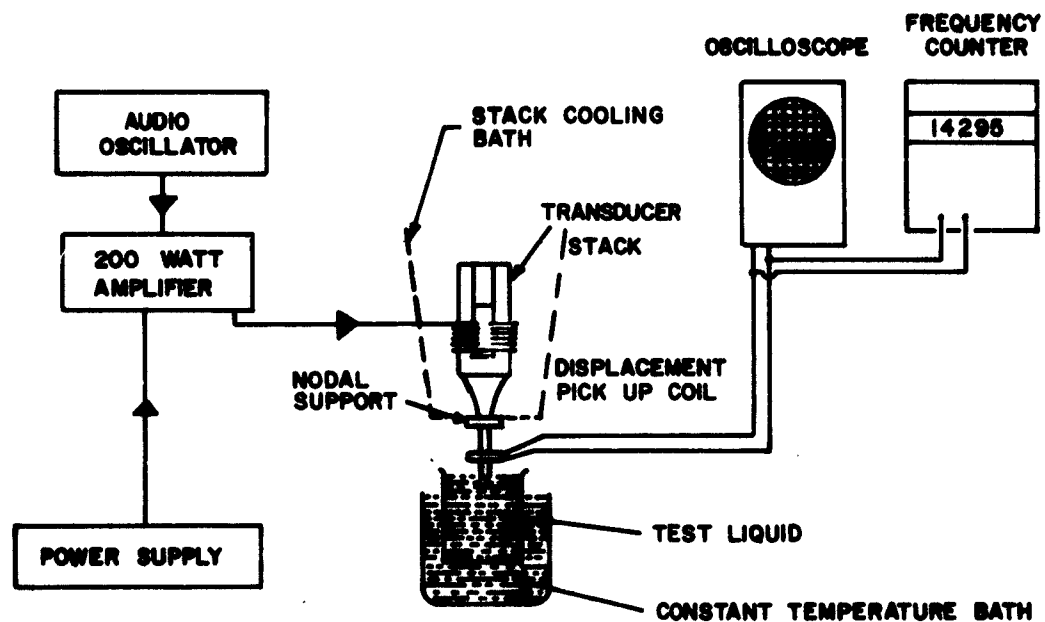
FIGURE I – BLOCK DIAGRAM OF THE MAGNETOSTRICTION APPARATUS USED FOR HIGH FREQUENCY FATIGUE TESTS
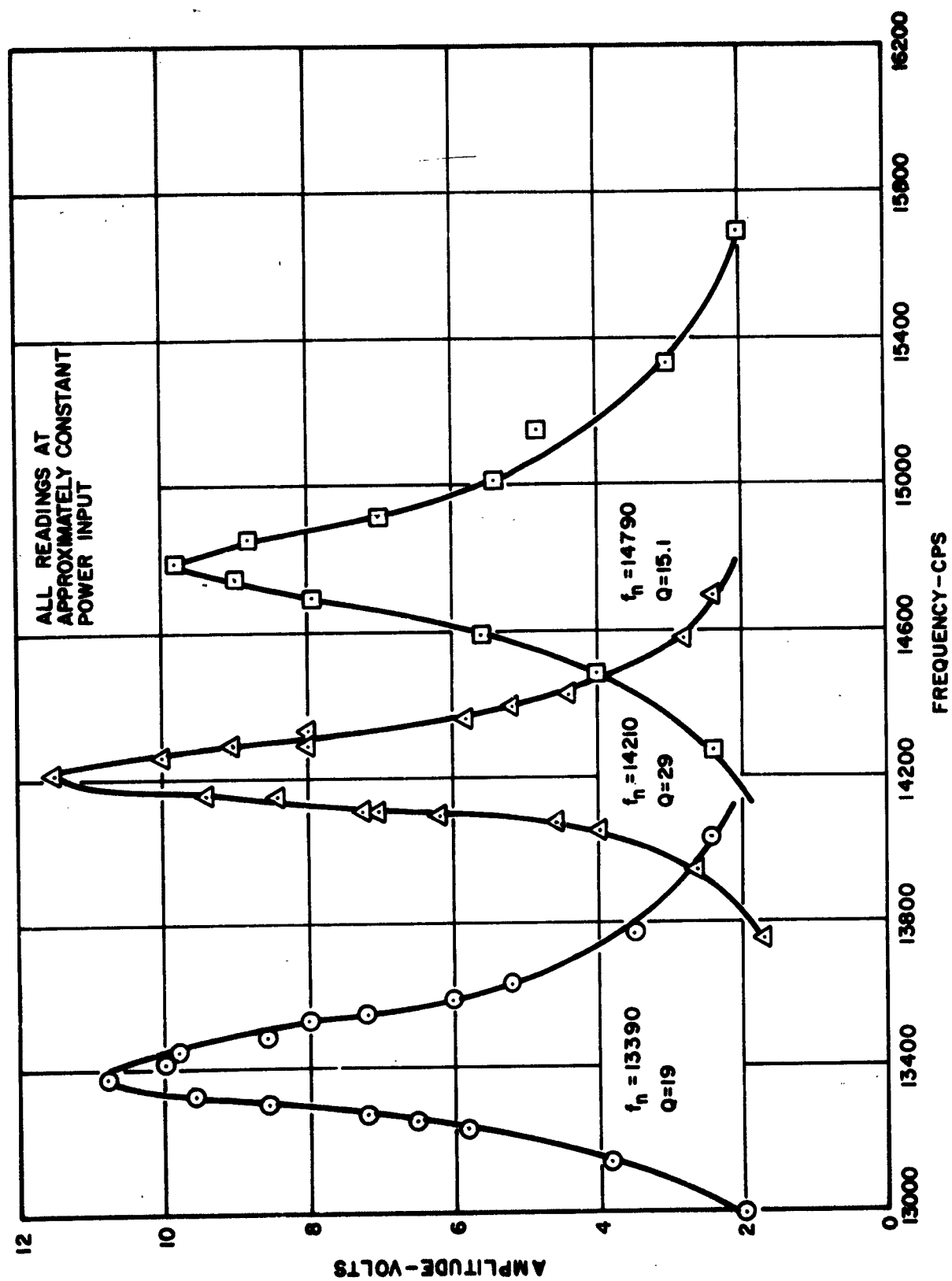
FIGURE 2 — TRANSDUCER CHARACTERISTICS

$$\epsilon_{max} = \frac{2\pi \cdot \xi_{max}}{\lambda}$$

STRAIN

ϵ_{max}

AMPLITUDE

ξ_{max}
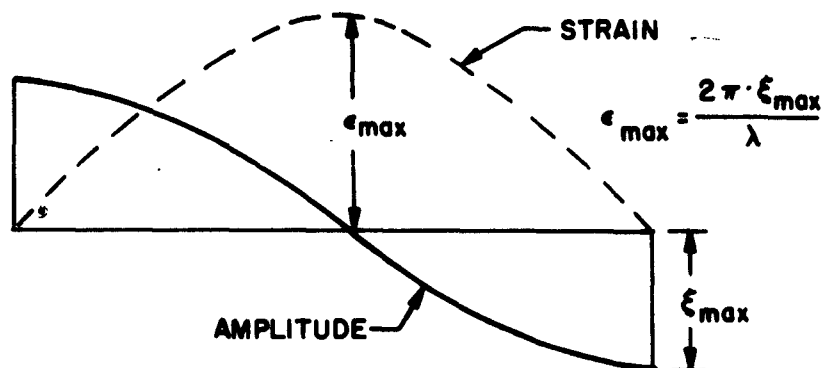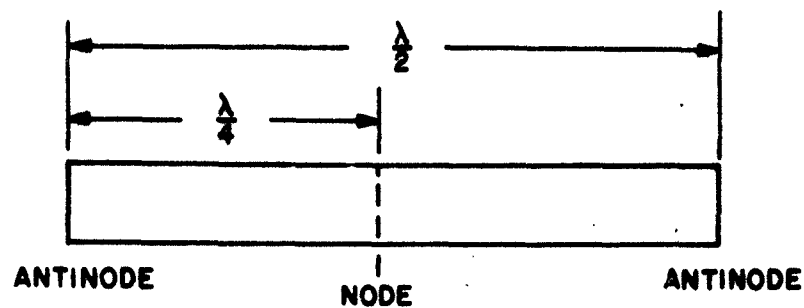
(a) UNNOTCHED HALF—WAVE LENGTH SPECIMEN

$$\epsilon'_{max} = M \epsilon_{max}$$

ϵ'_{max}

STRAIN

ϵ_{max}
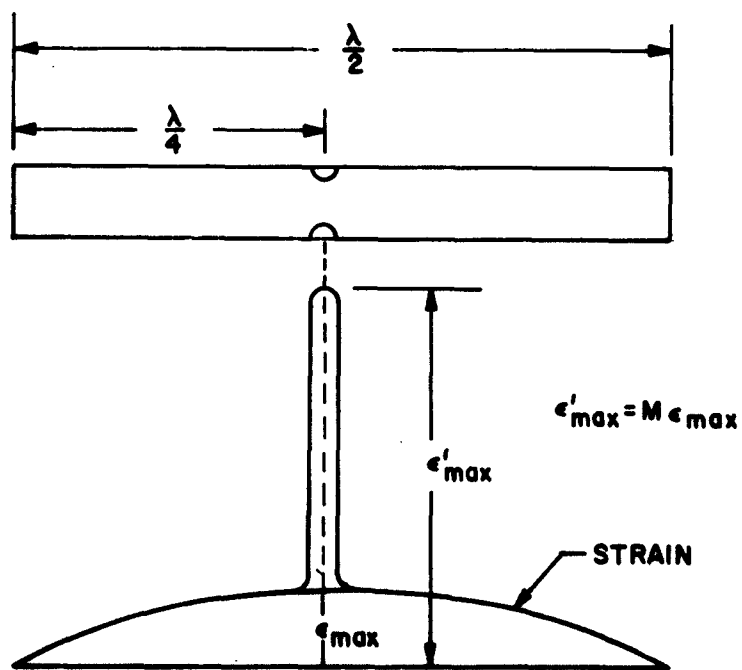
(b) NOTCHED HALF—WAVE LENGTH SPECIMEN

FIGURE 3 — BASIC PRINCIPLE OF HIGH FREQUENCY FATIGUE SPECIMEN DESIGN

ANTINODE   NODE   ANTINODE

$\frac{\lambda}{2}$

$\frac{\lambda}{4}$

NOTES:

1. GROOVE (DETAIL "A") IS TO BE SMOOTH, FREE FROM CHATTER TOOL MARKS, GROOVES OR OTHER DISCONTINUITIES. THE DIMENSIONS OF THE GROOVE MUST BE IDENTICAL FOR ALL SPECIMENS IN A LOT ± .001 AS MEASURED WITH AN OPTICAL COMPARATOR.

2. FINISH IN GROOVE 63 OR BETTER

3. DIMENSION "A" = HALF WAVE LENGTH OF SOUND
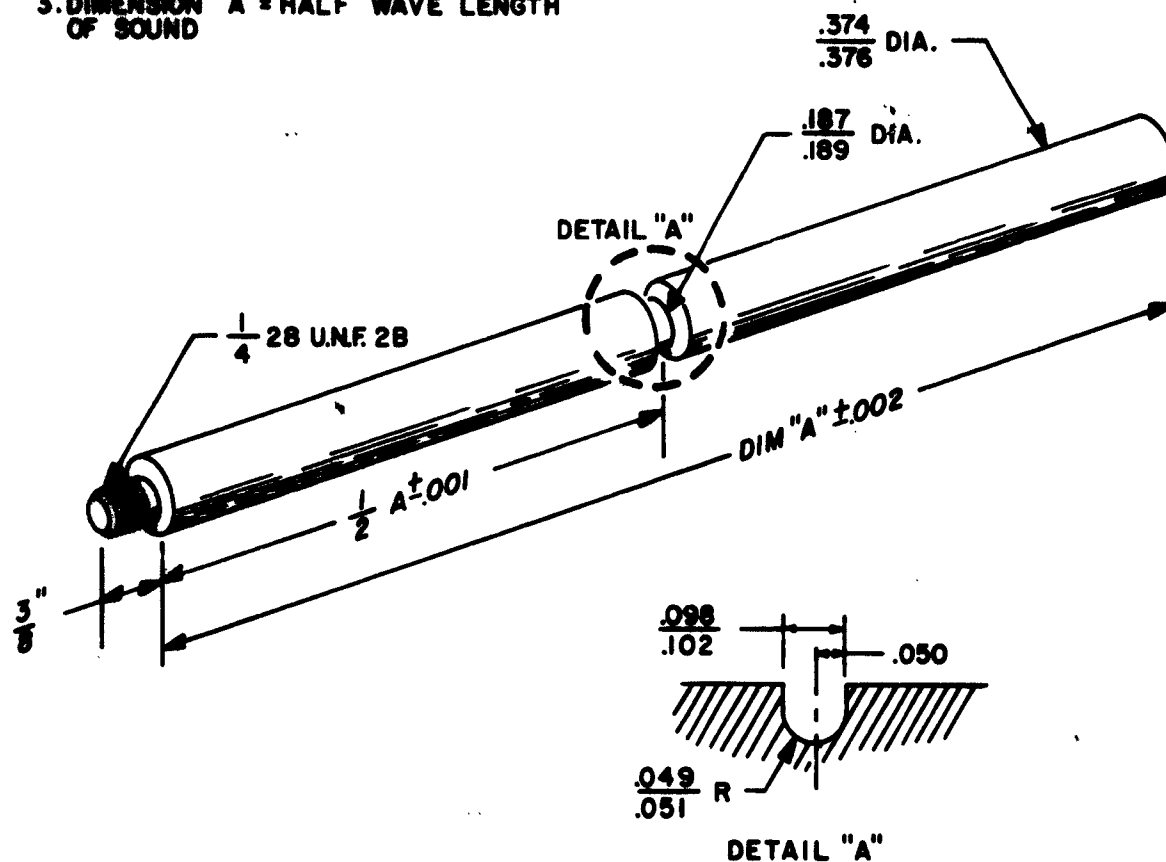
FIGURE 4(a) — HIGH FREQUENCY FATIGUE SPECIMEN
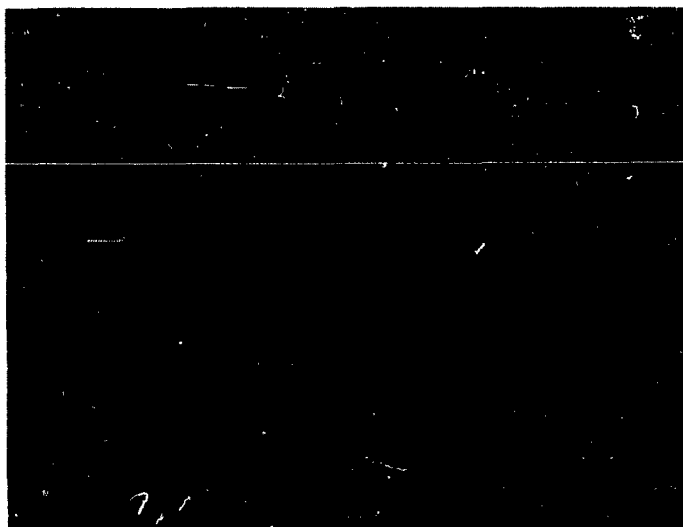
FIGURE 4 (b)-PHOTOGRAPH OF SAE 1020 STEEL FATIGUE SPECIMEN
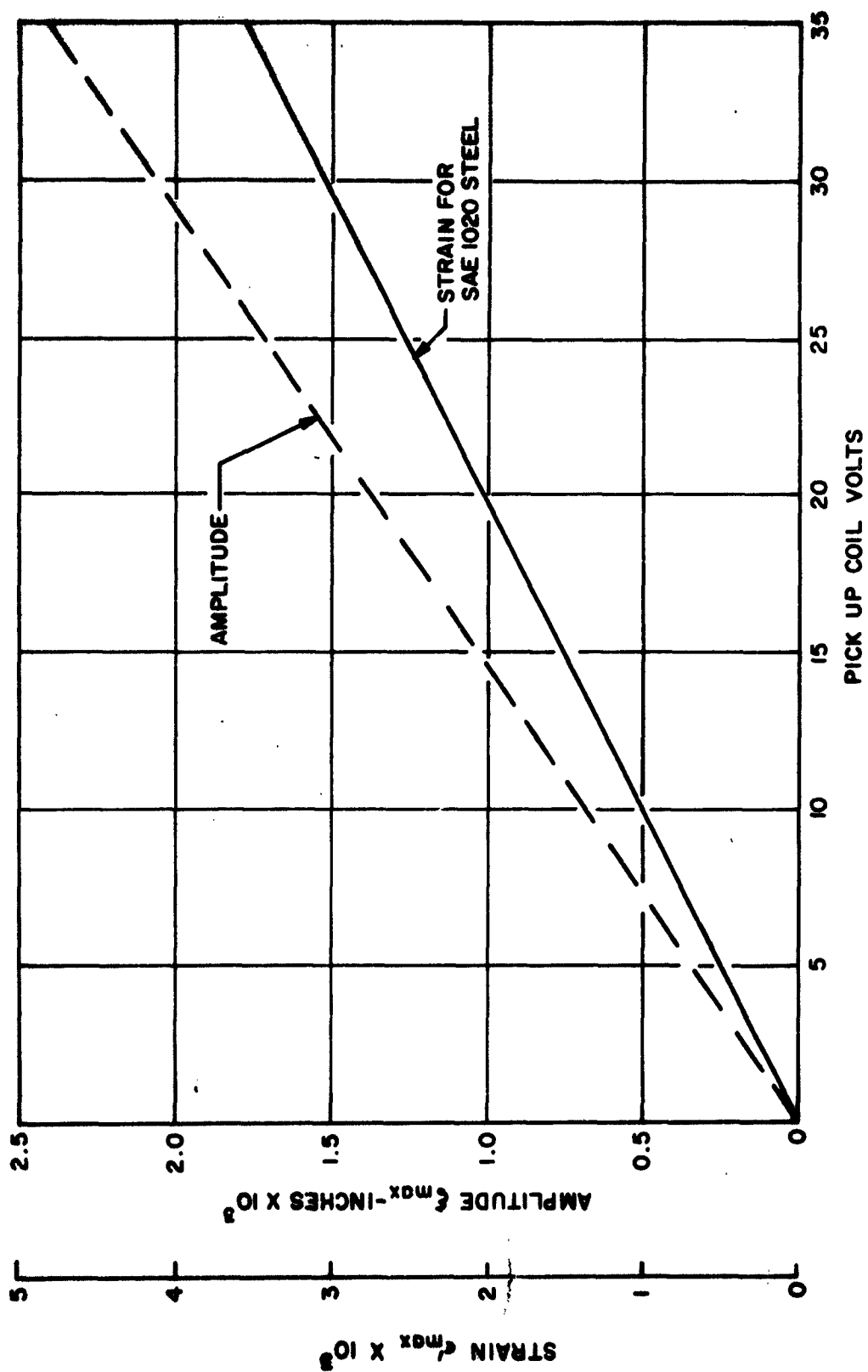
FIGURE 5 —CALIBRATION OF PICK UP COIL FOR MONITORING STRAINS
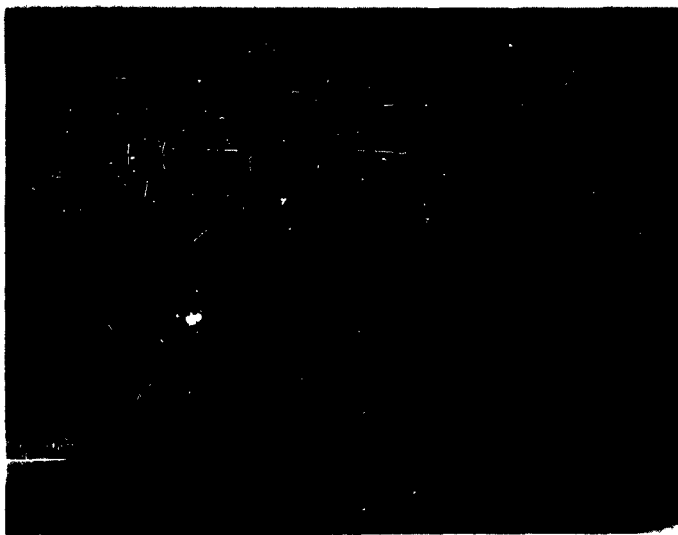
(a) OVERALL VIEW

(b) CLOSE UP OF SPECIMEN AND COOLING BATH

FIGURE 6 - GENERAL ARRANGEMENT OF HIGH FREQUENCY FATIGUE TESTING
APPARATUS
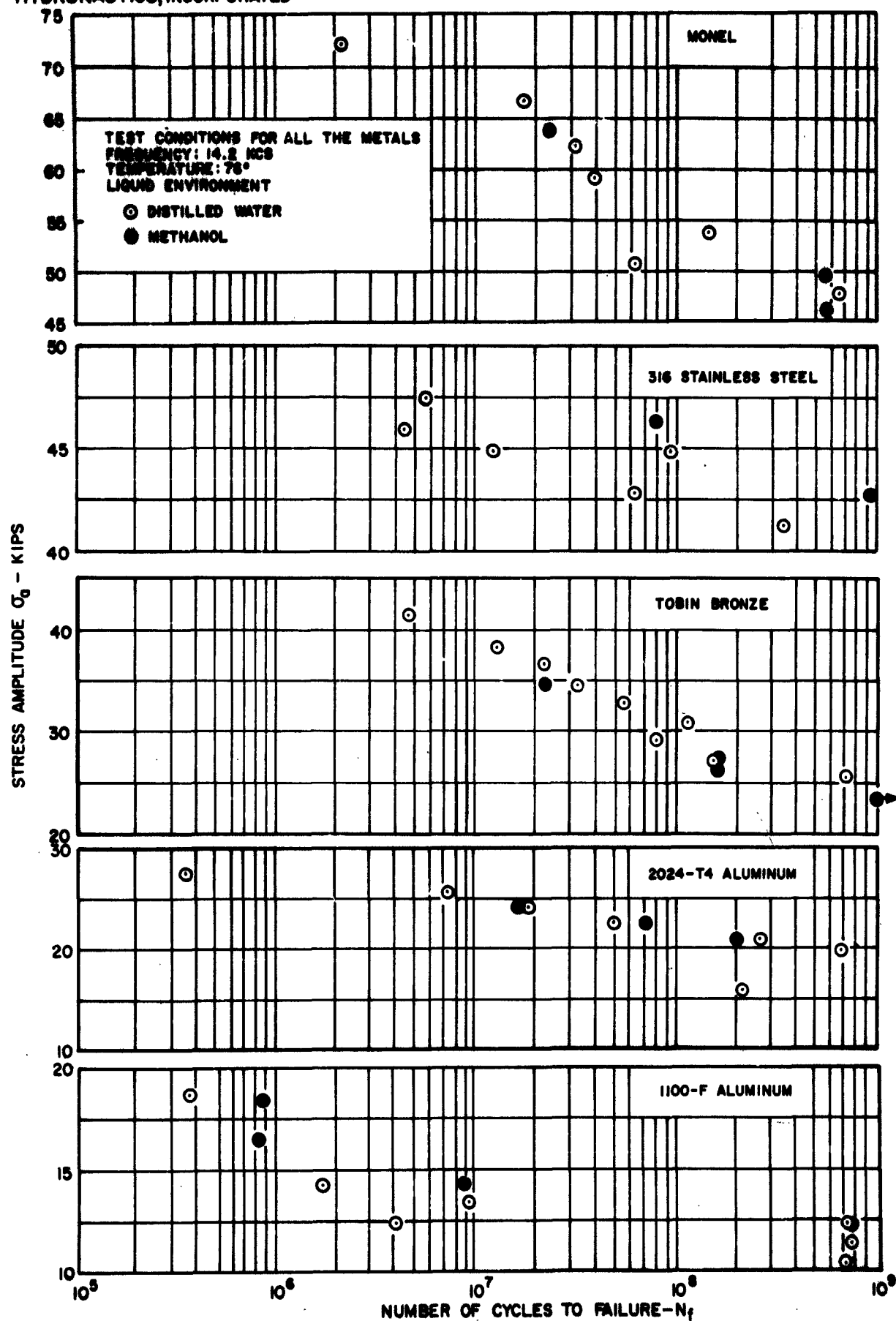
FIGURE 7 — RESULTS OF HIGH FREQUENCY FATIGUE TESTS

a) TYPICAL TRUE STRESS-STRAIN CURVE

b) LOGRITHMIC TRUE STRESS-STRAIN CURVE
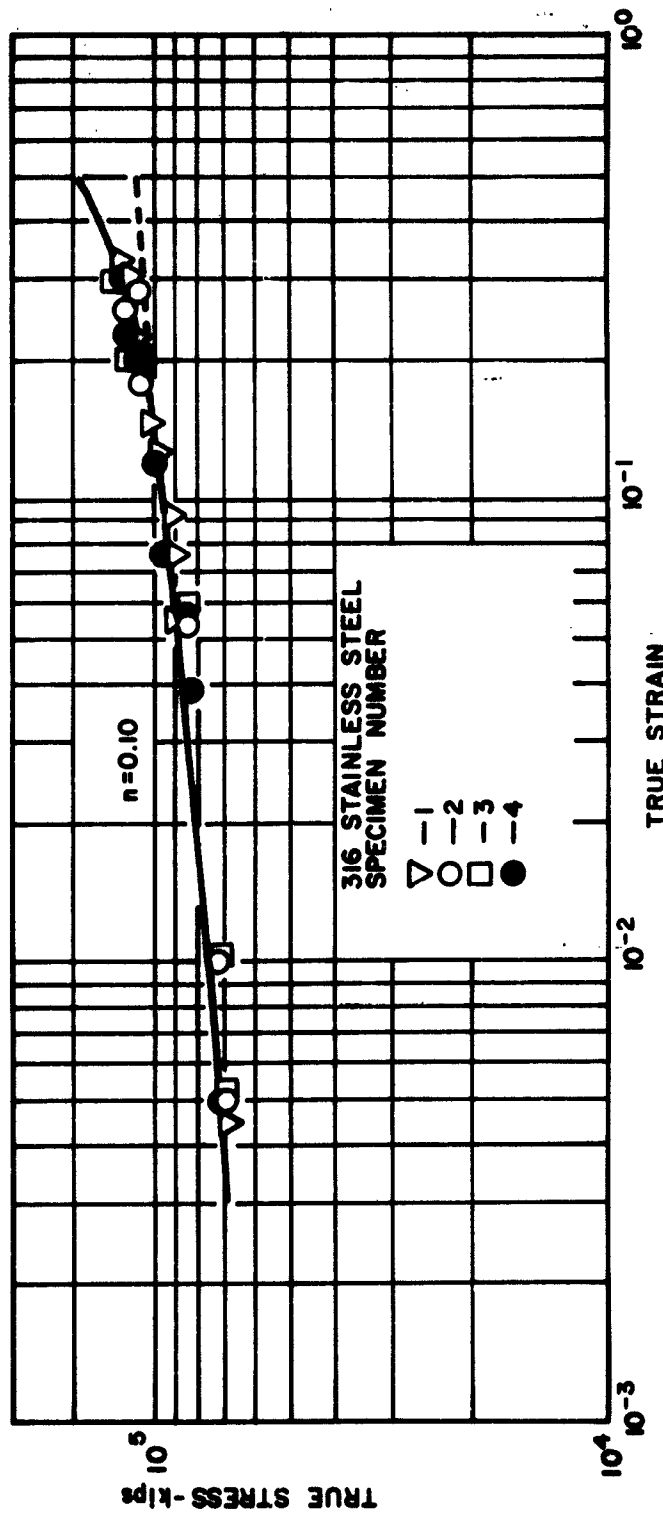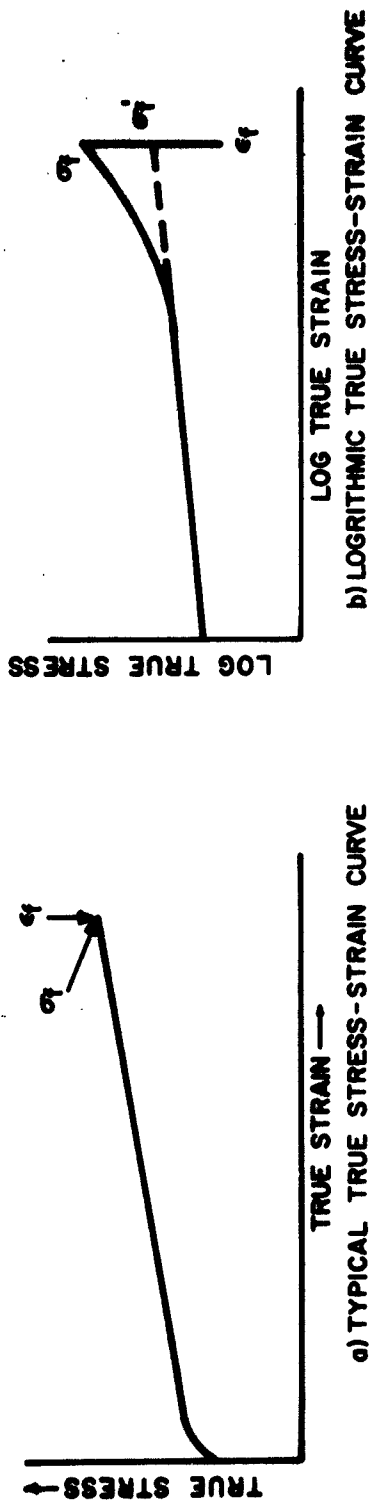
c) TRUE STRESS-STRAIN DATA FOR 316 STAINLESS STEEL

FIGURE 8 — TRUE STRESS-STRAIN CURVES

MONEL

○ DISTILLED WATER
● METHANOL

○ – 316 STAINLESS STEEL IN DISTILLED WATER
□ – 1100-F ALUMINUM IN DISTILLED WATER
◇ – TOBIN BRONZE IN DISTILLED WATER
▽ – 2024 ALUMINUM IN DISTILLED WATER
✳ – SHADED SYMBOL INDICATES METHANOL

LINES ARE COMPUTED FROM EQN (22) BY USING 85 % OF
THE STRAIN HARDENING EXPONENT.

LOG N_f

LOG f_o
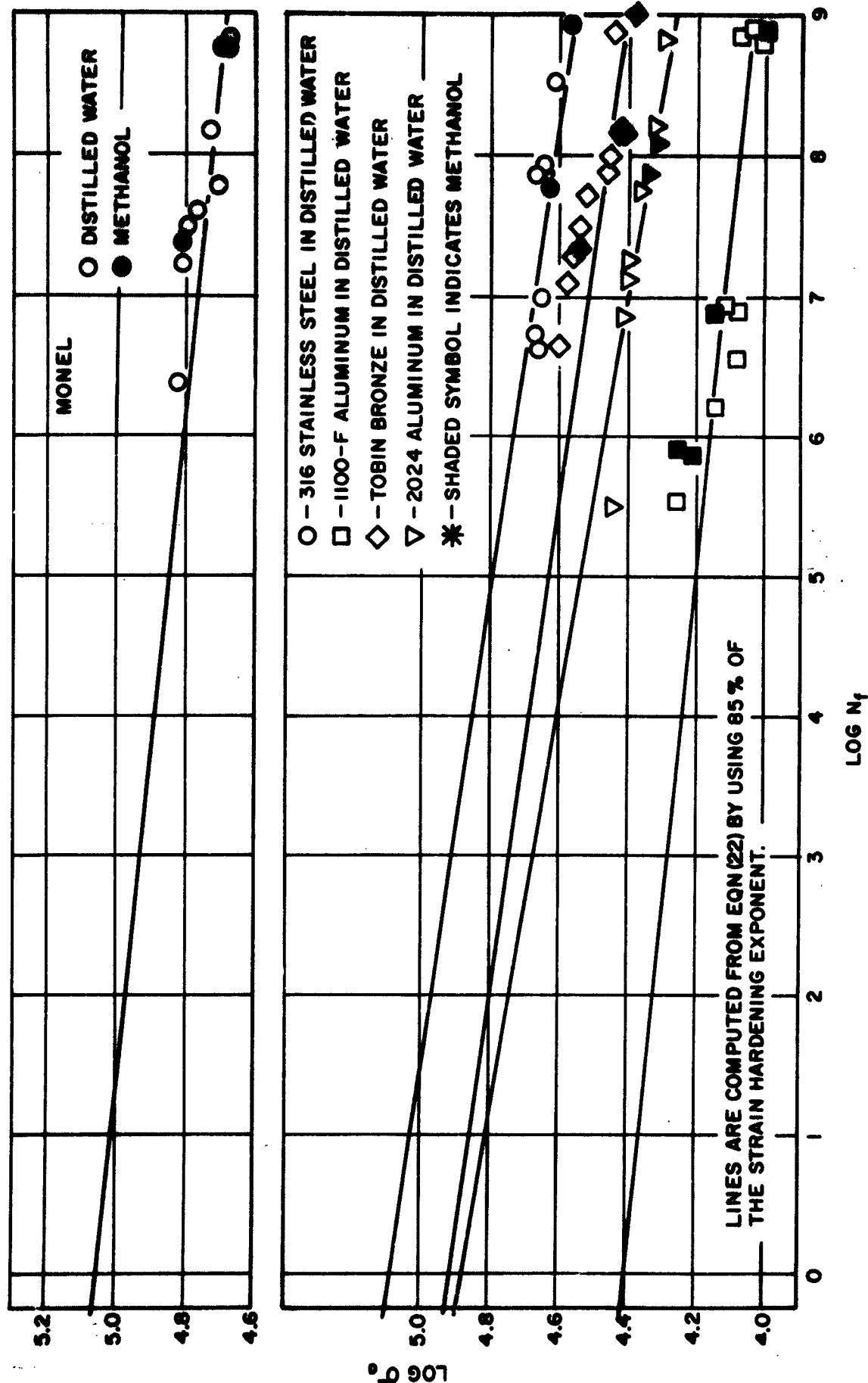
FIGURE 9 – COMPARISON BETWEEN THEORY AND HIGH FREQUENCY FATIGUE DATA
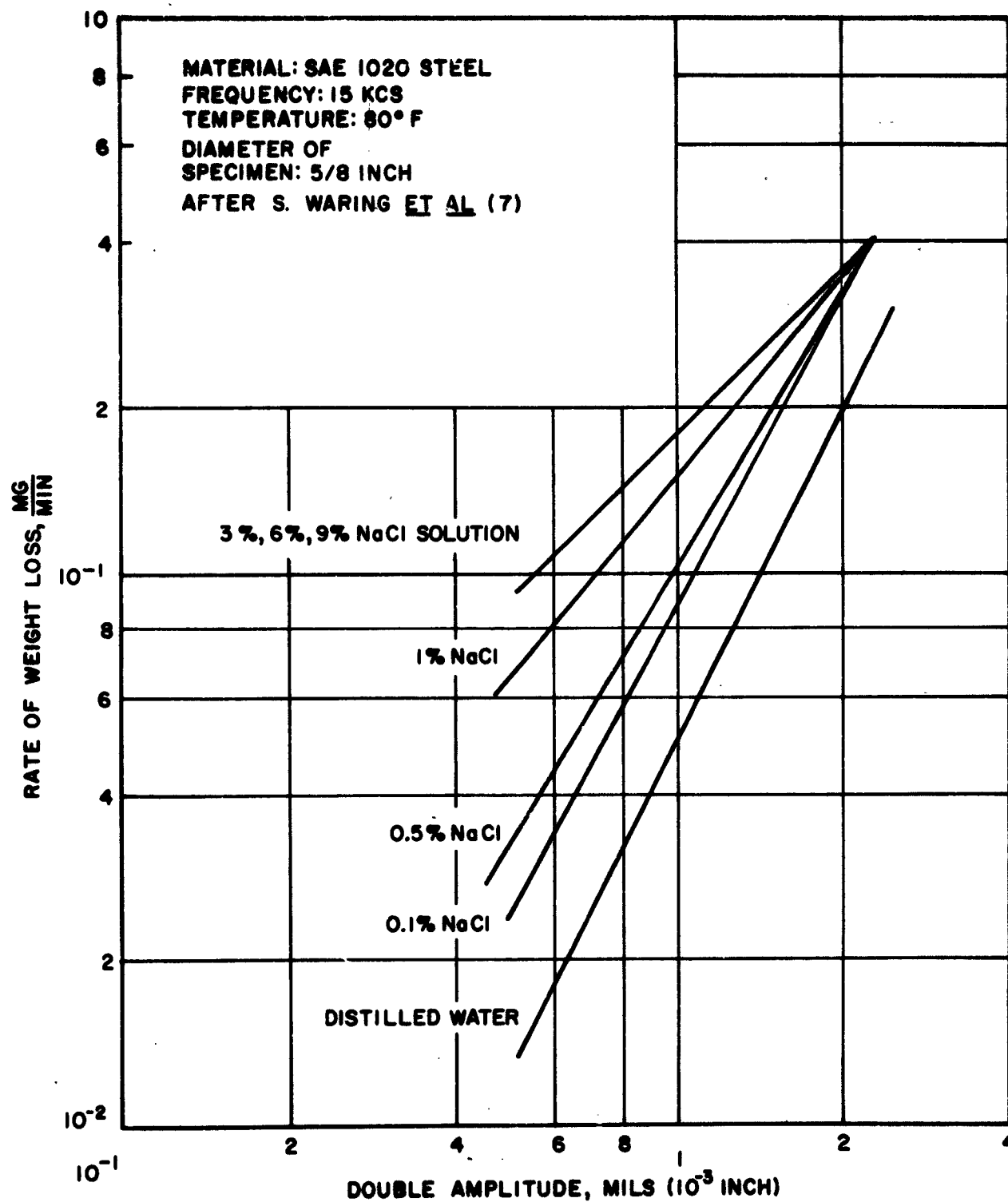
FIGURE 10 – EFFECT OF NaCl CONCENTRATION ON THE AMPLITUDE
VERSUS DAMAGE RATE RELATIONSHIP FOR SAE 1020 STEEL
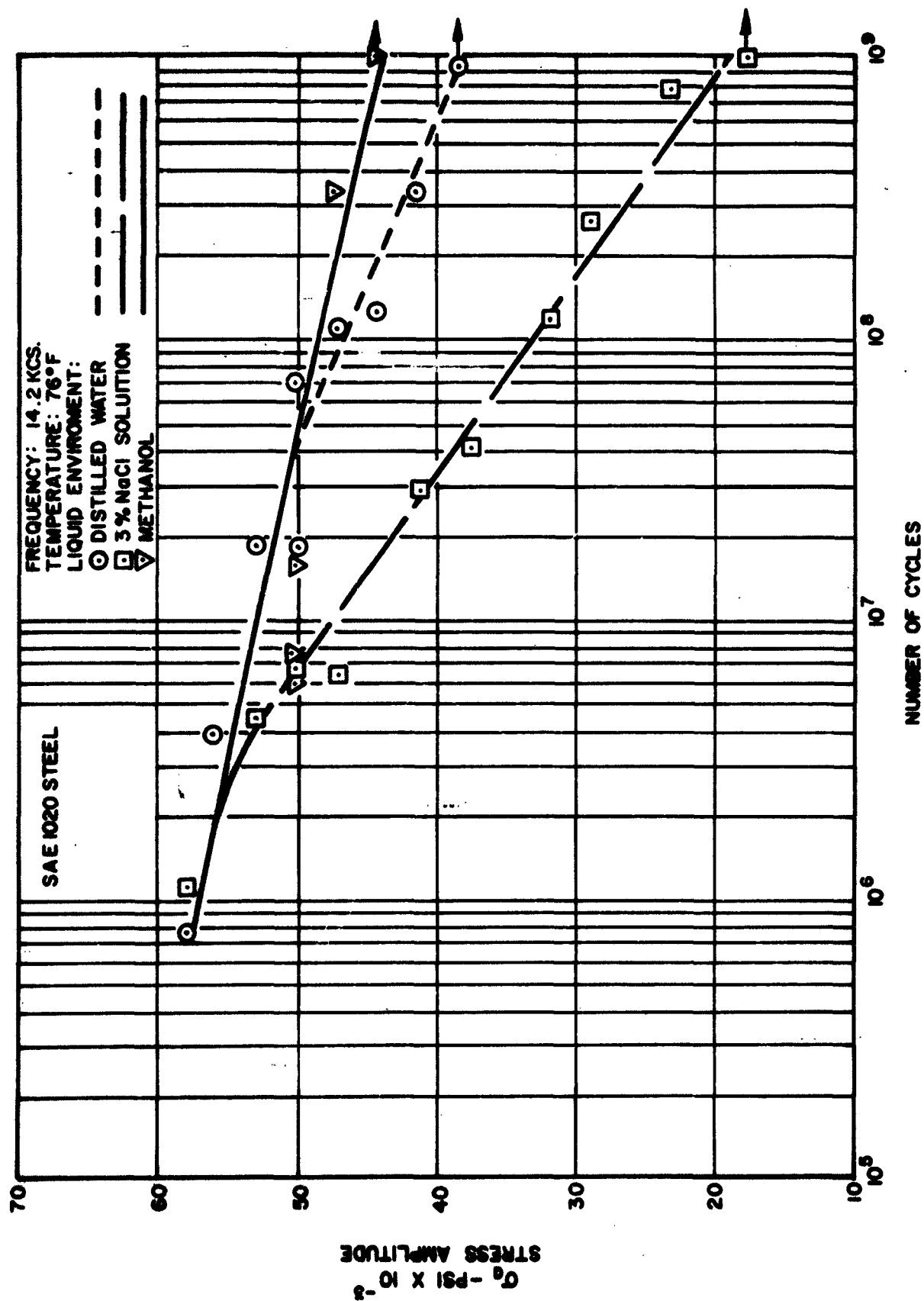
FIGURE II - HIGH FREQUENCY CORROSION FATIGUE OF SAE 1020 STEEL
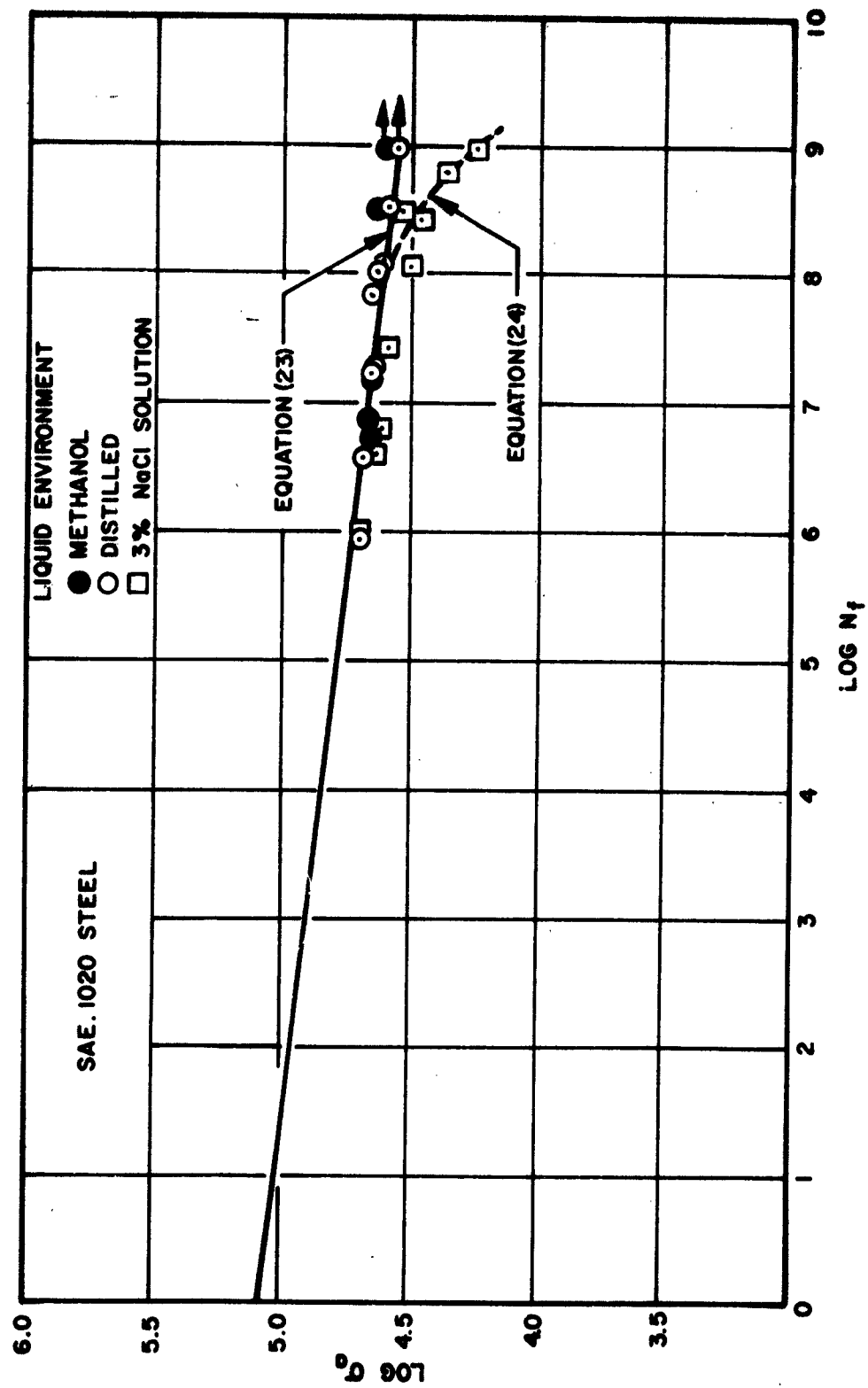
FIGURE 12 — CORROSION FATIGUE OF S.A.E. 1020 STEEL

DOCUMENT CONTROL DATA - R&D

(Security classification of title, body of abstract and indexing annotation must be entered when the overall report is classified)

1. ORIGINATING ACTIVITY (Corporate author)	2a. REPORT SECURITY CLASSIFICATION
AERONAUTICS Incorporated, Pindell School Road, Howard County, Laurel, Maryland	UNCLASSIFIED
	2b. GROUP

3. REPORT TITLE

HIGH FREQUENCY FATIGUE OF METALS AND THEIR CAVITATION DAMAGE RESISTANCE

4. DESCRIPTIVE NOTES (Type of report and inclusive dates)

Research Report

5. AUTHOR(S) (Last name, first name, initial)

Thiruvengadam, A.

6. REPORT DATE	7a. TOTAL NO. OF PAGES	7b. NO. OF REFS
December 1964	41	13

8a. CONTRACT OR GRANT NO.	9a. ORIGINATOR'S REPORT NUMBER(S)
Nonr 3755(00)FBM, NR 062-293	
b. PROJECT NO.	Technical Report 233-6
c.	9b. OTHER REPORT NO(S) (Any other numbers that may be assigned this report)
d.	

10. AVAILABILITY/LIMITATION NOTICES

Qualified requesters may obtain copies of this report from DDC.

11. SUPPLEMENTARY NOTES	12. SPONSORING MILITARY ACTIVITY
	Office of Naval Research

13. ABSTRACT

In order to verify the strain rate effects on the correlation between strain energy of metals and their cavitation damage resistance, high frequency fatigue tests at 14.2 kcs were conducted using a magnetostriction oscillator. Utilizing Morrow's theory, it has been shown that fatigue at this frequency can be quantitatively predicted if a fifteen percent reduction in static strain hardening factor is made. This result shows that strain rate effects are relatively small when plastic strain energy is used as a criterion.

Another result revealed by this study is the influence of corrosion. Present experiments show that fatigue strength can be reduced significantly for SAE 1020 steel in 3 percent NaCl solution even at high frequencies, thus confirming earlier speculations.

14.		LINK A		LINK B		LINK C	
KEY WORDS		ROLE	WT	ROLE	WT	ROLE	WT
Excitation Voltage							
High Frequency Fatigue							
Strain Energy							
Strain Rate Effects							
Corrosion Fatigue Factor							
Magnetostriction Oscillator							

INSTRUCTIONS

1. **ORIGINATING ACTIVITY:** Enter the name and address of the contractor, subcontractor, grantee, Department of Defense activity or other organization (*corporate author*) issuing the report.

2a. **REPORT SECURITY CLASSIFICATION:** Enter the overall security classification of the report. Indicate whether "Restricted Data" is included. Marking is to be in accordance with appropriate security regulations.

2b. **GROUP:** Automatic downgrading is specified in DoD Directive 5200.10 and Armed Forces Industrial Manual. Enter the group number. Also, when applicable, show that optional markings have been used for Group 3 and Group 4 as authorized.

3. **REPORT TITLE:** Enter the complete report title in all capital letters. Titles in all cases should be unclassified. If a meaningful title cannot be selected without classification, show title classification in all capitals in parenthesis immediately following the title.

4. **DESCRIPTIVE NOTES:** If appropriate, enter the type of report, e.g., interim, progress, summary, annual, or final. Give the inclusive dates when a specific reporting period is covered.

5. **AUTHOR(S):** Enter the name(s) of author(s) as shown on or in the report. Enter last name, first name, middle initial. If military, show rank and branch of service. The name of the principal author is an absolute minimum requirement.

6. **REPORT DATE:** Enter the date of the report as day, month, year; or month, year. If more than one date appears on the report, use date of publication.

7a. **TOTAL NUMBER OF PAGES:** The total page count should follow normal pagination procedures, i.e., enter the number of pages containing information.

7b. **NUMBER OF REFERENCES:** Enter the total number of references cited in the report.

8a. **CONTRACT OR GRANT NUMBER:** If appropriate, enter the applicable number of the contract or grant under which the report was written.

8b, 8c, & 8d. **PROJECT NUMBER:** Enter the appropriate military department identification, such as project number, subproject number, system numbers, task number, etc.

9a. **ORIGINATOR'S REPORT NUMBER(S):** Enter the official report number by which the document will be identified and controlled by the originating activity. This number must be unique to this report.

9b. **OTHER REPORT NUMBER(S):** If the report has been assigned any other report numbers (*either by the originator or by the sponsor*), also enter this number(s).

10. **AVAILABILITY/LIMITATION NOTICES:** Enter any limitations on further dissemination of the report, other than those imposed by security classification, using standard statements such as:

  (1) "Qualified requesters may obtain copies of this report from DDC."

  (2) "Foreign announcement and dissemination of this report by DDC is not authorized."

  (3) "U. S. Government agencies may obtain copies of this report directly from DDC. Other qualified DDC users shall request through

    _____ ."

  (4) "U. S. military agencies may obtain copies of this report directly from DDC. Other qualified users shall request through

    _____ ."

  (5) "All distribution of this report is controlled. Qualified DDC users shall request through

    _____ ."

If the report has been furnished to the Office of Technical Services, Department of Commerce, for sale to the public, indicate this fact and enter the price, if known.

11. **SUPPLEMENTARY NOTES:** Use for additional explanatory notes.

12. **SPONSORING MILITARY ACTIVITY:** Enter the name of the departmental project office or laboratory sponsoring (*paying for*) the research and development. Include address.

13. **ABSTRACT:** Enter an abstract giving a brief and factual summary of the document indicative of the report, even though it may also appear elsewhere in the body of the technical report. If additional space is required, a continuation sheet shall be attached.

It is highly desirable that the abstract of classified reports be unclassified. Each paragraph of the abstract shall end with an indication of the military security classification of the information in the paragraph, represented as (*TS*), (*S*), (*C*), or (*U*).

There is no limitation on the length of the abstract. However, the suggested length is from 150 to 225 words.

14. **KEY WORDS:** Key words are technically meaningful terms or short phrases that characterize a report and may be used as index entries for cataloging the report. Key words must be selected so that no security classification is required. Identifiers, such as equipment model designation, trade name, military project code name, geographic location, may be used as key words but will be followed by an indication of technical context. The assignment of links, roles, and weights is optional.

DD FORM 1 JAN 64 1473 (BACK)

HYDRONAUTICS, Incorporated

DISTRIBUTION LIST
(Contract Nonr 3755(00))

Chief of Naval Research
Department of the Navy
Washington 25, D. C.
Attn: Codes 438 3
   Code 461 1
     463 1
     429 1

Commanding Officer
Office of Naval Research
Branch Office
495 Summer Street
Boston 10, Massachusetts 1

Commanding Officer
Office of Naval Research
Branch Office
230 N. Michigan Avenue
Chicago 1, Illinois 1

Commanding Officer
Office of Naval Research
Branch Office
207 West 24th Street
New York 11, New York 1

Commanding Officer
Office of Naval Research
Branch Office
Navy No. 100, Box 39
Fleet Post Office
New York, New York 25

Commanding Officer
Office of Naval Research
Branch Office
1030 East Green Street
Pasadena 1, California 1

Commanding Officer
Office of Naval Research
Branch Office
1000 Geary Street
San Francisco 9, California 1

Director
U.S. Naval Research Laboratory
Washington 25, D. C.
Attn: Codes 2000 1
     2020 1
     2027 6

Chief, Bureau of Ships
Department of the Navy
Washington 25, D. C.
Attn: Codes 300 1
     305 1
     335 1
     341 1
     342A 1
     345 1
     421 1
     440 1
     442 1
     634A 1
Attn: Code 634 (B. Taylor) 1
   Code 634 (L. Birnbaum) 1

Chief, Bureau of Naval Weapons
Department of the Navy
Washington 25, D. C.
Attn: Codes R 1
     R-12 1
     RR 1
     RRRE 1
     RU 1
     RUTO 1

Chief, Bureau of Yards and Docks
Department of the Navy
Washington 25, D. C.
Attn: Codes D-202   1
              D-400   1
              D-500   1

Commanding Officer and Director
David Taylor Model Basin
Washington 7, D. C.
Attn: Codes 142   1
              500   1
              513   1
              521   1
              526   1
              550   1
              563   1
              589   1
   Dr. M. Strasberg (901)   1

Commander
U.S. Naval Ordnance Laboratory
Silver Spring, Maryland
Attn: Dr. A. May   1
          Desk DA   1
          Desk HL   1
          Desk DR   1

Commander
U.S. Naval Ordnance Test Station
China Lake, California
Attn: Codes 5014   1
              4032   1
              753   1

Hydrographer
U.S. Navy Hydrographic Office
Washington 25, D. C.   1

Commander
U.S. Naval Ordnance Test Station
Pasadena Annex
3202 E. Foothill Boulevard
Pasadena 8, California
Attn: Mr. J. W. Hoyt   1
          Research Division   1
          P508   1
          P804   1
          P807   1
          P80962 (Library)   1
          Mr. J. W. Hicks   1

Superintendent
U. S. Naval Academy
Annapolis, Maryland
Attn: Library   1

Commanding Officer and Director
U. S. Navy Marine Engineering
Laboratory
Annapolis, Maryland 21402
Attn: Code 750   1

Commander
U. S. Naval Weapons Lab.
Dahlgren, Virginia
Attn: Tech. Library Div.   1
          Computation and Exterior
          Ballistics Laboratory
          (Dr. Hershey)   1

Commanding Officer
NROTC and Naval Administrative
Unit
Massachusetts Institute of Tech.
Cambridge 39, Massachusetts   1

Commanding Officer and Director
U.S. Underwater Sound Laboratory
Fort Trumbull
New London, Connecticut
Attn: Technical Library   1

HYDRONAUTICS, Incorporated

-3-

Commanding Officer and Director
U.S. Navy Mine Defense Laboratory
Panama City, Florida   1

Superintendent
U.S. Naval Postgraduate School
Monterrey, California
Attn: Library   1

Commanding Officer and Director
U.S. Naval Electronic Laboratory
San Diego 52, California
Attn: Code 4223   1

Commanding Officer and Director
U.S. Naval Civil Engineering Lab.
Port Hueneme, California   1

New York Naval Shipyard
Material Laboratory
Brooklyn, 1, New York
Attn: Mr. C. K. Chatten
        Code 949   1

Commander
Norfolk Naval Shipyard
Portsmouth, Virginia   1

Commander
New York Naval Shipyard
U. S. Naval Base
Brooklyn, New York   1

Commander
Boston Naval Shipyard
Boston 29, Massachusetts   1

Commander
Philadelphia Naval Shipyard
U. S. Naval Base
Philadelphia 12, Penn.   1

Commander
Portsmouth Naval Shipyard
Portsmouth, New Hampshire
Attn: Design Division   1

Commander
Charleston Naval Shipyard
U. S. Naval Base
Charleston, South Carolina   1

Commanding Officer
U. S. Naval Underwater
Ordnance Station
Newport, Rhode Island
Attn: Research Division   1

Commander
Long Beach Naval Shipyard
Long Beach 2, California   1

Commander
Pearl Harbor Naval Shipyard
Navy No. 128, Fleet Post Office
San Francisco, California   1

Commander
San Francisco Naval Shipyard
San Francisco 24, California   1

Shipyard Technical Library
Code 303TL, Bldg. 746
Mare Island Naval Shipyard
Vallejo, California   1

Superintendent
U. S. Merchant Marine Academy
Kings Point, Long Island,
New York
Attn: Dept. of Engr.   1

Commandant, U. S. Coast Guard
1300 E. Street, N. W.
Washington, D. C.   1

HYDRONAUTICS, Incorporated

-4-

Beach Erosion Board
U. S. Army Corps of Engineers   1
Washington 25, D. C.

Commanding Officer
U. S. Army Research Office
Box CM, Duke Station
Durham, North Carolina   1

Commander
Hdqs. U.S. Army Transportation
Research and Development Command
Transportation Corps
Fort Eustis, Virginia   1

Director
U. S. Army Engineering Research
and Development Laboratories
Fort Belvoir, Virginia
Attn: Tech. Documents Center   1

Office of Technical Services
Department of Commerce
Washington 25, D. C.   1

Defense Documentation Center
Cameron Station
Alexandria, Virginia   10

Maritime Administration
441 G. Street, N. W.
Washington 25, D. C.
Attn: Coordinator of Research   1
      Div. of Ship Design   1

Fluid Mechanics Section
National Bureau of Standards
Washington 25, D. C.
Attn: Dr. G. B. Schubauer   1

U.S. Atomic Energy Commission
Technical Information Service
Extension, P. O. Box 62
Oak Ridge, Tennessee   1

Scientific and Technical
Information Facility
Attn: NASA Representative
P. O. Box 5700
Bethesda, Maryland 20014   1

Director
Langley Research Center
National Aeronautics and
Space Administration
Langley Field, Virginia   1

Director
Ames Research Laboratory
National Aeronautics and
Space Administration
Moffett Field, California   1

National Aeronautics and
Space Administration
Lewis Research Center
21000 Brookpark Road
Cleveland, Ohio 44135
Attn: Director   1
      Mr. Cavour H. Hauser   1
      Mr. James P. Couch   1

Director
Engineering Science Division
National Science Foundation
Washington, D. C.   1

Commander
Air Force Cambridge Research
Center, 230 Albany Street,
Cambridge 39, Massachusetts
Attn: Geophysical Research
      Library   1

Air Force Office of Scientific
Research, Mechanics Division
Washington 25, D. C.   1

HYDRONAUTICS, Incorporated

National Research Council
Montreal Road
Ottawa 2, Canada
Attn: Mr. E. S. Turner   1

Engineering Societies Library
29 West 39th Street
New York 18, New York   1

Society of Naval Architects and
Marine Engineers
74 Trinity Place
New York 6, New York   1

Webb Institute of Naval
Architecture
Glen Cove, Long Island, New York
Attn: Prof. E. V. Lewis   1
           Technical Library   1

The John Hopkins University
Baltimore 18, Maryland
Attn: Prof.S. Corrsin   1
         Prof. F.H. Clauser   1
         Prof. O. M. Phillips   1

Director
Applied Physics Laboratory
The John Hopkins University
8621 Georgia Avenue
Silver Spring, Maryland   1

New York State University
Maritime College
Engineering Department
Fort Schuyler, New York
Attn: Prof. J. J. Foody   1

California Institute of Tech.
Pasadena 4, California
Attn: Hydrodynamics Lab.
         Prof. T. Y. Wu   1
         Prof. A. Ellis   1
         Prof. A. Costa   1
         Prof. M. Plesset   1

University of California
Berkeley 4, California
Attn: Department of Engineering
         Prof. H. A. Schade   1
         Prof. J. Johnson   1
         Prof. J. V. Wehausen   1
         Prof. E. V. Laitone   1
         Prof. P. Lieber   1
         Prof. M. Holt   ,   1

University of California
Los Angeles, California
Attn: Prof. R. W. Leonard   1
         Prof. A. Powell   1

Director
Scripps Institution of Oceanography
University of California
La Jolla, California   1

Iowa Institute of Hydraulic Research
State University of Iowa
Iowa City, Iowa
Attn: Prof. H. Rouse   1
         Prof. L. Landweber   1
         Prof. P. G. Hubbard   1

Harvard University
Cambridge 38, Massachusetts
Attn: Prof. G. Birkhoff   1
         Prof. S. Goldstein   1

University of Michigan
Ann Arbor, Michigan
Attn; Engineering Research
     Institute   1
     Prof. F.G. Hammitt
     (Dept. of Nuclear Engr.) 1

Director
Ordnance Research Laboratory
Pennsylvania State University
University Park, Pennsylvania
Attn: Dr. G. F. Wislicenus 1

Director
St. Anthony Falls Hydraulic Lab.
University of Minnesota
Minneapolis 14, Minnesota
Attn: Mr. J. N. Wetzel 1
     Prof. B. Silberman 1
     Prof. L. G. Straub 1

Massachusetts Institute of
Technology
Cambridge 39, Massachusetts
Attn: Prof. P. Mandel 1
     Prof. M. A. Abkowitz 1

Institute for Fluid Mechanics
and Applied Mathematics
University of Maryland
College Park, Maryland
Attn: Prof. J. M. Burgers 1

Cornell Aeronautical Laboratory
Buffalo 21, New York
Attn: Mr. W. F. Milliken, Jr. 1

Brown University
Providence 12, Rhode Island
Attn: Dr. R. E. Meyer 1
     Dr. W. H. Reid 1

Stevens Institute of Technology
Davidson Laboratory
Hoboken, New Jersey
Attn: Mr. D. Savitsky 1
     Mr. J. P. Breslin 1
     Dr. D. N. Hu 1
     Dr. S. J. Lukasik 1

Director
Woods Hole Oceanographic Inst.
Woods Hole, Massachusetts 1

Director
Alden Hydraulic Laboratory
Worcester Polytechnic Institute
Worcester, Massachusetts 1

Stanford University
Stanford, California
Attn: Dr. Byrne Perry
     (Dept. of Civil Engr.) 1
     Prof. E. Y. Hsu
     (Dept. of Civil Engr.) 1
     Dr. S. Kline
     (Dept. of Mech. Engr.) 1

Dr. E.R.G. Eckert
Mechanical Engineering Department
University of Minnesota
Minneapolis, Minnesota 55455 1

Department of Theoretical and
Applied Mechanics
College of Engineering
University of Illinois
Urbana, Illinois
Attn: Dr. J. M. Robertson 1

Department of Mathematics
Rensselaer Polytechnic Institute
Troy, New York
Attn: Prof. R. C. DiPrima 1

Southwest Research Institute
8500 Culebra Road
San Antonio 6, Texas
Attn: Dr. H.N. Abramson   1

Department of Aeronautical Engr.
University of Colorado
Boulder, Colorado
Attn: Prof. M.S. Uberoi   1

Courant Institute
New York University
New York, New York
Attn: Prof. P. Garabedian   1

Institut fur Schiffbau der
Universitat Hamburg
Lammersieth 90
Hamburg 33, Germany
Attn: Prof. O. Grim   1
      Prof. K. Wieghardt   1

Max-Planck Institut fur
Stromungsforschung
Bottingerstrasse 6-8
Gottingen, Germany
Attn: Dr. H. Reichardt, Dir.   1

Versuchsanstalt fur Wasserbau
und Schiffbau
Gartenufer (Schleuseninsel)
1 Berlin 12, Germany
Attn: Prof. Dr. Ing.S.Schuster 1

Netherlands Ship Model Basin
Wageningen, The Netherlands
Attn: Ir. R. Wereldsma   1
      Dr. J.B. Van Manen   1

Mitsubishi Shipbuilding and
Engineering Company
Nagasaki, Japan
Attn: Dr. K. Taniguchi   1

Mr. W.R. Wiberg, Chief
Marine Performance Staff
The Boeing Company
Aero-Space Division
P. O. Box 3707
Seattle 24, Washington   1

Mr. William P. Carl
Grumman Aircraft Corporation
Bethpage, L.I., New York   1

Grumman Aircraft Corporation
Bethpage, L.I., New York
Attn: Engineering Library
      Plant 5   1
      Mr. Leo Geyer   1

Mr. G. W. Paper
ASW and Ocean Systems Dept.
Lockheed Aircraft Corporation
Burbank, California   1

Dr. A. Ritter
Therm Advanced Research Div.
Therm, Incorporated
Ithaca, New York   1

HYDRONAUTICS, Incorporated
Pindell School Road
Howard County
Laurel, Maryland
Attn: Mr. P. Eisenberg
      (President)   1
      Mr. M.P. Tulin
      (Vice President)   1

Dr. J. Kotik
Technical Research Group, Inc.
Route 110
Melville, New York   1

AiResearch Manufacturing Co.
9851-9951 Sepulveda Boulevard
Los Angeles 45, California
Attn: Blaine R. Parkin   1

Hydrodynamics Laboratory
Convair
San Diego 12, California
Attn: Mr. H.E. Brooke   1
       Mr. R. H. Oversmith   1

Baker Manufacturing Company
Evansville, Wisconsin   1

Gibbs and Cox, Inc.
21 West Street
New York 16, New York   1

Electric Boat Division
General Dynamics Corporation
Groton, Connecticut
Attn: Mr. R. McCandliss   1

Mr. A. Grindell
Oak Ridge National Laboratory
Oak Ridge, Tennessee   1

ITT Research Institute
10 W. 35th Street
Chicago 16, Illinois   1

Missile Development Division
North American Aviation, Inc.
Downey, California
Attn: Dr. E. R. Van Driest   1

National Physical Laboratory
Teddington, Middlesex, England
Attn: Head, Aerodynamics Div.
       Mr. A. Silverleaf   1

Aerojet General Corporation
6352 N. Irwindale Avenue
Azusa, California
Attn: Mr. C.A. Gongwer   1

Astropower, Inc.
2121 Paularino Avenue
Newport Beach, California
Attn: R. D. Bowerman   1

Transportation Technical
Research Institute
No. 1057-1-Chome
Mejiro-machi, Toshima-ku
Tokyo-to, Japan   1

Oceanics, Incorporated
Plainview, Long Island, N.Y.
Attn: Dr. Paul Kaplan   1

Director, Special Projects Office
Department of the Navy
Washington 25, D. C.
Attn: Code SP-001   1

National Academy of Sciences
National Research Council
Committee on Undersea Warfare
2101 Constitution Avenue
Washington 25, D. C.   1

Dr. Harvey Brooks
School of Applied Sciences
Harvard University
Cambridge, Massachusetts   1